



CHORUS

This is the accepted manuscript made available via CHORUS. The article has been published as:

Spin-polarized multiexcitons in quantum dots in the presence of spin-orbit interaction

A. H. Russ, L. Schweidenback, M. Yasar, C. H. Li, A. T. Hanbicki, M. Korkusinski, G. Kioseoglou, B. T. Jonker, and A. Petrou

Phys. Rev. B **84**, 045312 — Published 15 July 2011

DOI: [10.1103/PhysRevB.84.045312](https://doi.org/10.1103/PhysRevB.84.045312)

Spin-polarized multi-excitons in quantum dots in the presence of spin-orbit interaction

A.H. Russ¹, L. Schweidenback¹, M. Yasar¹, C.H. Li², A.T. Hanbicki², M. Korkusinski³,
G. Kioseoglou^{2,4,*}, B.T. Jonker², A. Petrou¹

¹*Department of Physics, University at Buffalo, Buffalo, New York 14260, USA*

²*Naval Research Laboratory, Washington, District of Columbia, 20375, USA*

³*Quantum Theory Group, Institute for Microstructural Sciences, National Research Council, Ottawa, Canada K1A0R6*

⁴*Department of Materials Science and Technology, University of Crete, Heraklion Crete, 71003, Greece*

Abstract

An efficient electron spin-relaxation mechanism has been observed in InAs quantum dots (QDs) that manifests itself as a sharp drop in the circular polarization of the light emitted by Fe spin-light emitting diodes, which incorporate a single layer of InGaAs QDs, for a narrow range of magnetic fields around 5 tesla. The underlying mechanism occurs when the QDs are occupied by three electron-hole pairs forming a tri-exciton (3X) and is a two step process. The first step involves the spin flip of one of the three electrons mediated by the spin-orbit interaction; in the second step the 3X relaxes to its ground state via phonon emission.

* electronic mail: gnk@materials.uoc.gr

I. Introduction

Semiconductor quantum dots (QDs) are potentially important components for many spintronic and quantum computing applications such as spin-transistors, spin filters and spin memory devices because it is possible to effectively inject, manipulate, and read-out spins in these systems¹. One particularly enabling property of QDs is enhanced spin lifetimes. The zero dimensional character of QDs results in the quantization of the electronic orbital states, which significantly suppresses many spin flip mechanisms and leads to long spin-relaxation times². This effect has been seen in several experiments including electrical spin injection into self assembled InGaAs QDs using ferromagnetic GaMnAs, paramagnetic ZnMnSe and ZnBeMnSe layers, as well as ferromagnetic metal contacts³⁻¹². Room temperature electrical spin pumping has also been achieved¹⁰ and it has been attributed to the suppression of the Dyakonov-Perel spin relaxation mechanism. In addition to enhanced spin lifetimes, QDs are useful tools to understand the basic physics of spin manipulation in low dimensions. Indeed, we have recently shown that it is possible to electrically control the electron population and spin polarization of the QD shells with bias current and have experimentally determined values for the s-p and p-d exchange energies¹².

In this work we present an efficient magnetic field induced spin relaxation mechanism for electrons injected into InGaAs QDs. We use QD spin-light emitting diode (LEDs) with an Fe injector as a platform to effectively inject and detect spins, as well as a means to investigate spin relaxation in several multi-exciton configurations. The magnetic contact acts as the source of spin-polarized electrons while the bias on the diode controls the number of excitons present in the dots. We have studied the magnetic field

dependence of the circular polarization of the light emitted by the spin-LEDs in the range of 5-60K. In a narrow range of magnetic fields around 5 Tesla, there is a dramatic decrease in optical polarization superimposed on the saturation polarization. These results are interpreted as the optical signature of spin relaxation mediated by the spin-orbit interaction; we propose a model that describes a possible efficient electron spin relaxation mechanism to interpret our results.

II. Experimental

The samples used in this study were grown by molecular beam epitaxy (MBE) in interconnected growth chambers on *p*-GaAs (001) substrates. They are *n*-*i*-*p* structures with the following dimensions: 2000 Å *p*-GaAs buffer/500 Å *p*-Al_{0.3}Ga_{0.7}As barrier/ 400 Å undoped GaAs QW /830 Å *n*-Al_{0.1}Ga_{0.9}As barrier. A 100 Å thick Fe(001) film was then grown in a separate MBE chamber at a substrate temperature below 5 °C to minimize potential intermixing at the Fe/Al_{0.1}Ga_{0.9}As interface. The top 150 Å of *n*-type Al_{0.1}Ga_{0.9}As barrier was highly doped ($n = 1 \times 10^{19} \text{ cm}^{-3}$) to form a Schottky tunnel contact in order to facilitate spin injection from the Fe film^{13, 14}.

Different InAs QD layers were embedded at the center of the undoped GaAs QW region. Sample 1 was grown at a rate of 0.03 ML/sec with a high QD density ($5 \times 10^{10} \text{ cm}^{-2}$) and a broad QD size distribution with diameters ranging from 100-250 Å. For sample 2 on the other hand, the InAs QD layer was grown at a lower rate of 0.001 ML/sec. A much lower QD density ($7 \times 10^8 / \text{cm}^2$) is obtained by terminating the growth at the onset of dot formation. The significantly reduced growth rate also results in a more narrow size

distribution (average diameter 400-500 Å). In both samples the QD height is equal to 35 Å. The s-p sub-level spacing in both samples is the same and equal to 45 meV.

The samples were processed to form surface emitting LEDs using standard photolithography and chemical etching techniques. Devices were measured in a variable temperature optical magnet cryostat, where the magnetic field was applied along the z -axis perpendicular to the device layers (xy -plane). The emitted light was collected in the Faraday geometry and was dispersed by a single monochromator equipped with a multichannel charge coupled device (CCD) detector. The electroluminescence (EL) spectra were analyzed into their σ^+ (LCP) and σ^- (RCP) components using a combination of quarter wave plate and linear polarizer placed before the spectrometer entrance slit.

III. Results and Discussion

A typical EL spectrum from Sample 1 at $I = 5$ mA, $T = 7$ K and zero magnetic field is shown as an inset in Fig. 1. Because of the broad size distribution of sample 1, the p-shell is not resolved in the EL spectrum. However, at higher currents, when the spectrum is deconvoluted it clearly contains two features (s- and p-shell) separated by 45 meV, which is the same as for sample 2. Also presented in Fig. 1 is the circular polarization, P_{circ} , for the same sample at $T=7$ K plotted as a function of the magnetic field B . P_{circ} is defined as $P_{circ} = [I(\sigma^+) - I(\sigma^-)] / [I(\sigma^+) + I(\sigma^-)]$, where $I(\sigma^\pm)$ is the intensity of the positive or negative helicity component (measured at the EL intensity maximum). The circular polarization increases as function of B tracking the out of plane magnetization of the Fe film but instead of saturating after $2.2T^{13}$, P_{circ} exhibits a sharp decrease for a range of magnetic fields centered at $\pm 5T$. This “resonance” has a FWHM

of ~ 1 T and a strong temperature dependence. The bias dependence of the circular polarization for sample 1 is shown in Fig. 2a. It is clear that as we increase the bias, the observed drop of the polarization degree around 5 T is suppressed. We attribute this to the dependence of the spin-orbit interaction Hamiltonian on the p-n junction electric field E . It is strong for low bias voltage, and thus strong E . That would indicate that the spin-orbit interaction is described by the Rashba Hamiltonian¹⁵. The model that we discuss below allows for either the Rashba or Dresselhaus Hamiltonian for inhomogeneous QDs. Plots of P_{circ} vs. B for positive fields are shown in Fig. 2b for $T = 7, 15, 30, 45,$ and 50 K. When the sample temperature is raised, the resonance is suppressed and practically vanishes by $T = 50$ K. These data suggest that, for $T < 50$ K, there exists an efficient magnetic field induced spin relaxation mechanism for electrons injected into the QDs. We interpret this behavior as the optical signature of spin relaxation mediated by spin-orbit interaction.

Injection of spin-polarized electrons into the optically active QD layer leads to the formation of multiexciton complexes with spin-polarized electrons^{12, 16}. The majority of the injected electrons are in the spin-down state, and therefore the emission spectra associated with recombination of these electrons with unpolarized holes are predominantly left circularly polarized (σ_+). In a system of N electron-hole pairs, typically the excited states are spin-polarized, while the ground state has a low-spin character, a consequence of the so-called hidden symmetries in the electronic properties of exciton systems confined in quantum dots¹⁷. Relaxation from the highly polarized, excited state to the ground, low polarization ground state requires a spin flip process, and therefore cannot be carried out by phonon emission. This is the reason why the polarized

states are long-lived, and result in a consistent polarization of emitted photons over a wide range of magnetic fields. However, the experiment described in this work demonstrates that there exists a narrow range of magnetic fields, where the polarization of the emitted light is drastically reduced, suggesting that under these conditions spin-flip relaxation process becomes efficient.

We attribute this polarization loss to an electron spin-flip process mediated by the spin-orbit interaction. Since the energy scale of this interaction is typically very small (several hundreds of μeV)¹⁸, such transition can only occur if the high and low spin multiexciton complex levels have comparable energies. Such resonance conditions are achieved by tuning the energies of the low- and high-spin states by an externally applied magnetic field. Once the system undergoes a transition to its low-spin state, it can relax to the ground state by emitting a phonon.

IV. Theoretical model

We describe this process by approximating the self-assembled InAs QD by a two-dimensional harmonic oscillator (HO) potential. The single-particle electron energies in this potential, in the presence of the magnetic field $\vec{B} = (0, 0, B)$, are

$$E^{(e)}(n_e, m_e) = \hbar\Omega_+^{(e)}\left(n_e + \frac{1}{2}\right) + \hbar\Omega_-^{(e)}\left(m_e + \frac{1}{2}\right), \quad \text{where } n_e, m_e = 0, 1, 2, \dots \text{ are the}$$

quantum numbers, $\Omega_{\pm}^{(e)} = \Omega_h^{(e)} \pm \Omega_c^{(e)} / 2$, $\Omega_h^{(e)} = \sqrt{\Omega_0^{(e)2} + \Omega_c^{(e)2} / 4}$ is the hybrid energy,

$\Omega_0^{(e)}$ is the electron oscillator energy, $\Omega_c^{(e)} = eB / m_e^*c$ is the cyclotron energy, e and m_e^* is the electron charge and effective mass, respectively, and c is the speed of light. The

single-particle hole energies are expressed analogously, but scaled by the hole oscillator energy $\Omega_0^{(h)}$ and effective mass m_h^* (we only consider the heavy hole subband). In the following we express all energies in terms of the effective Rydberg $1Ry = m_e^* e^4 / 2\varepsilon^2 \hbar^2$ and all distances in terms of the effective Bohr radius $1a_B = \varepsilon \hbar^2 / m_e^* e^2$ with ε being the dielectric constant of the QD material. For InAs $m_e^* = 0.054m_0$ and $\varepsilon = 12.4$; this gives $1Ry = 4.78meV$ and $1a_B = 12.2nm$. For model calculations we take $\Omega_0^{(e)} = 7.32Ry = 35meV$ and $\Omega_0^{(h)} = 3.66Ry = 17.5meV$, as determined from the experimental inter-shell energy spacings¹². The single-particle states $|n, m, \sigma\rangle$ are additionally labeled by the spin projection $\sigma_e = \pm 1/2$ for electrons (henceforth denoted as \uparrow and \downarrow , respectively) and $\sigma_h = \pm 3/2$ for holes ($\uparrow\uparrow$ and $\downarrow\downarrow$, respectively). Under the symmetry conditions $m_e^* \Omega_0^{(e)} = m_h^* \Omega_0^{(h)}$ the wave functions of an electron and a hole labeled by the same indices are identical, and in what follows we assume that $m_h^* = 0.108m_0$. The single-particle wave functions are characterized by the electron and hole angular momenta $l^{(e)} = n_e - m_e$ and $l^{(h)} = m_h - n_h$, respectively. The total angular momentum L of an electron-hole pair is $L = l^{(e)} + l^{(h)}$.

We consider single-particle states populated by N interacting electron-hole pairs. The Hamiltonian of such a system, expressed in terms of the electron creation (annihilation) operators c_i^+ (c_i) on state $i = \{n_e, m_e, \sigma_e\}$ and analogous hole creation (annihilation) operators h_j^+ (h_j) on state $j = \{n_h, m_h, \sigma_h\}$ has the form:

$$\begin{aligned}
H = & \sum_i E^{(e)}(i) c_i^\dagger c_i + \sum_j E^{(h)}(j) h_j^\dagger h_j + \frac{1}{2} \sum_{ijkl} \langle ij | V_{ee} | kl \rangle c_i^\dagger c_j^\dagger c_k c_l \\
& + \frac{1}{2} \sum_{ijkl} \langle ij | V_{hh} | kl \rangle h_i^\dagger h_j^\dagger h_k h_l - \sum_{ijkl} \langle ij | V_{eh} | kl \rangle c_i^\dagger h_j^\dagger h_k c_l.
\end{aligned}$$

The first two terms of this Hamiltonian describe the single-particle energies of the carriers. The remaining terms account for the electron-electron, hole-hole, and electron-hole interactions, respectively¹⁷. In the HO basis with the electron-hole symmetry discussed above, the matrix elements defined by the same set of indices are equal in magnitude and can be expressed by a magnetic-field dependent interaction constant

$$V_0 = \sqrt{\pi \Omega_h^{(e)}}.$$

The spin-orbit interaction Hamiltonian can be expressed as the sum

$$H_{SO} = H_{SO}^{(D)} + H_{SO}^{(R)} \text{ where } H_{SO}^{(D)} \text{ is the Dresselhaus Hamiltonian } -\frac{\beta}{\hbar} (\hat{\sigma}_x \hat{\pi}_x - \hat{\sigma}_y \hat{\pi}_y) \text{ and}$$

$$H_{SO}^{(R)} \text{ is the Rashba Hamiltonian } -\frac{\alpha}{\hbar} (\hat{\sigma}_x \hat{\pi}_y - \hat{\sigma}_y \hat{\pi}_x), \text{ with } \hat{\sigma} = (\hat{\sigma}_x, \hat{\sigma}_y, \hat{\sigma}_z) \text{ being the Pauli}$$

operators, and $\hat{\pi} = \hat{p} - \frac{e}{c} \vec{A}$ being the generalized momentum in a magnetic field

described by the vector potential \vec{A} . The constants α and β scaling the above terms are typically of the order of several $\text{meV} \cdot \text{\AA}$, giving the spin-orbit interaction the energy scale of several hundreds of μeV ¹⁸. Given the energy scale of the single-particle and Coulomb interaction Hamiltonians (tens of meV), we treat the spin-orbit interaction as a perturbation.

A detailed analysis of the N electron-hole pair system in the presence of the spin-orbit interaction involves first computing the properties of the unperturbed exciton systems as already outlined in Ref. [16]. To this end we prepare all possible

configurations of the electrons and holes with a definite total angular momentum and total projection of the electron and hole spins, write the Hamiltonian matrix in the basis of these configurations, and diagonalize the Hamiltonian numerically. Once the eigenstates of the unperturbed Hamiltonian are known, we account for the spin-orbit interaction between states, which for a given magnetic field are very close in energy. Details of this procedure, as well as an extensive discussion of the results will be presented elsewhere. Here we will give a simplified description that allows us to understand the principles of the proposed model.

We start with a discussion of the three-exciton (3X) complex and assume for simplicity that the 3X states can be expressed in terms of single configurations. **Starting with the 3X system may seem an arbitrary choice but the proposed model considers energy configurations close enough for spin-orbit assisted transitions to be effective and thus account for the observed decrease of the optical polarization. In sample 1 we have a mixture of occupancies i.e. 1X, 2X, 3X but as will be discussed later, for the 1X and 2X complexes, such resonances take place at very high magnetic fields. Thus only the resonance associated with the 3X complex falls within the range of fields we have used in our experiments.** The ground low spin state of such a system in the presence of a magnetic field, $|A\rangle = c_{00\uparrow}^+ c_{01\downarrow}^+ c_{00\downarrow}^+ h_{00\uparrow}^+ h_{01\uparrow}^+ h_{00\downarrow}^+ |0\rangle$, is shown schematically in Fig. 3(a). The expectation value E_A of the unperturbed interacting Hamiltonian is equal to $\langle A|H|A\rangle = 3\Omega_h^{(e)} + \Omega_-^{(e)} + 3\Omega_h^{(h)} + \Omega_-^{(h)} - 3.1875V_0$. This state is a low spin state with the unpaired electron and hole occupying the p shell. Under the polarized injection conditions of our work we expect that the system will be in a long-lived high spin state $|B\rangle = c_{10\downarrow}^+ c_{01\downarrow}^+ c_{00\downarrow}^+ h_{00\uparrow}^+ h_{01\uparrow}^+ h_{00\downarrow}^+ |0\rangle$, as is shown schematically in Fig. 3(b). Its energy

$E_B = 5\Omega_h^{(e)} + 3\Omega_h^{(h)} + \Omega_-^{(h)} - 3.375V_0$ contains a larger total kinetic energy than configuration A, but is renormalized by a larger negative interaction term due to the fact that the electrons are distributed individually across single-particle orbitals and are spin polarized. In our analysis a key role will be played by yet another configuration, $|C\rangle = c_{01\uparrow}^+ c_{01\downarrow}^+ c_{00\downarrow}^+ h_{00\uparrow}^+ h_{01\uparrow}^+ h_{00\downarrow}^+ |0\rangle$, schematically shown in Fig. 3(c). Its energy, $E_C = 3\Omega_h^{(e)} + 2\Omega_-^{(e)} + 3\Omega_h^{(h)} + \Omega_-^{(h)} - 2.9375V_0$, has a somewhat lower kinetic energy component, but it is also renormalized by a less negative interaction term.

In Fig. 4 we compare the energies of the three states plotted as a function of magnetic field. As can be seen, at zero magnetic field configuration B is lower in energy than C, but at some field value the energies of these two configurations cross. On the other hand, the ground-state configuration A is always at much lower energy than the other two. Configuration B is considered due to the fact that spin polarized electrons are injected into the QDs, as already discussed above, leading to a definite polarization of the emitted light. The central aspect in this analysis is that for the critical magnetic field of about 4.75 T, configurations B and C are close enough in energy for a spin-orbit assisted transition to occur between these two states. For the range of magnetic fields around 4.75 T for which the energies of states B and C are near-degenerate, spin-polarized configuration B can significantly mix with the spin-unpolarized, excited configuration C. After mixing, the system can relax efficiently to the ground-state configuration A. Since the 3X system now assumes a low spin state, the photons emitted in radiative recombination of carriers are expected to have low average polarization. At magnetic field values above and below 4.75 T the two excited states B and C are farther apart in

energy, and their coupling by the spin-orbit interaction decreases. As a result, the spin-polarized configuration B is stable, resulting in the reappearance of polarized emission.

Below we analyze the mixing of configurations B and C in more detail. The angular momenta of these two configurations differ by $\Delta L = L_B - L_C = 2$, and the total electronic spin projection difference is $\Delta\sigma_e = -1$. The spin-orbit interaction can only mix states differing by one unit of angular momentum and one unit of spin. Specifically, the Rashba term decreases the angular momentum by one unit while raising the spin by one (or vice versa). The Dresselhaus term on the other hand increases (or decreases) both the angular momentum and spin by one. Therefore for an isotropic quantum dot, configurations B and C will not be mixed by the spin-orbit interaction. However, any anisotropy in the dots will result in a strong mixing of the two excited single-particle states by spin-orbit interaction, since angular momentum is no longer a good quantum number. The energy relaxation from state C to state A proceeds via phonon emission. We note that in our samples the energy separation between states C and A at 4.75 T is equal to 36 meV which is very close to the LO interface phonon mode in InAs QDs embedded in GaAs¹⁹. Therefore efficient relaxation from state C to state A can occur by the emission of a single phonon.

We conclude our analysis by considering a similar mechanism for the system of two electron-hole pair (2X) and single electron-hole pair (1X) excitons. The ground state A of the 2X system, shown schematically in Fig. 5(a), consists of four carriers occupying the lowest single-particle states in a spin-unpolarized configuration. Spin-polarized injection of electrons leads to the formation of state B depicted in Fig. 5(b), in which the spins of the two electrons are aligned, and one of the electrons is promoted to the p shell.

We do not find any candidate low spin excited state which would come to resonance with this spin polarized configuration. The only possible spin-orbit assisted transition could take place between the unpolarized ground state A and the fully spin-polarized configuration C shown in Fig. 5(c). However, such a configuration becomes the ground state of the system at magnetic fields in excess of 100 Tesla. Therefore no polarization quenching effect is expected for the polarized biexciton 2X for the relatively low magnetic field values used in our experiment.

In the case of a single electron-hole pair (1X), when the first excited QD state crosses the second excited state, a sharp drop in the spin lifetime has been predicted^{20, 21}. If we use $\Omega_0^{(e)} = 35\text{meV}$ and $\Omega_0^{(h)} = 17.5\text{meV}$ the magnetic field required is well above the values used in our experiment. Even if we assume a g-factor of 14 (the value for bulk InAs)²² the crossing occurs at 23 T. In reality the g-factors in InAs QDs are smaller²³ which means the resonant field would be even higher. Thus the single electron-hole pair exciton scenario is also excluded.

The three electron-hole model is compatible with the temperature dependence of the resonance strength shown in Fig.2. At elevated temperatures the average phonon population increases and interferes with the relaxation from state C to state A which requires phonon emission.

V. Testing the Model

We have investigated the predictions of the model discussed above by studying sample 2, which has a lower QD density and a narrow lateral size distribution. Unlike

sample 1, in sample 2 we can resolve EL features due to recombination among the various shells of the QDs, and we can thus determine the average occupancy of the QD ensemble. In this sample we see a gradual filling of the shells as the diode current is increased¹². The zero field EL spectrum for sample 2 at average occupancy $N = 3$ is shown in Fig.6 (no detector response correction was applied). Assuming that the oscillator strengths of the s- and p-shell recombination channels are approximately equal, we adjusted the device current so that the corrected intensity of the p-shell EL feature is half that of the s-shell feature. For higher (lower) currents the average occupancy is above (below) 3. In Fig.7 (a) we plot the polarization of the s-shell EL feature as function of magnetic field B at $N > 3$. The polarization increases monotonically with field following the out-of-plane magnetization, and saturates above 2.5 T. In Fig.7(b) we show the same plot for average occupancy $N = 3$. The P_{circ} versus B plot in this case exhibits a clear resonance centered around 4.5 T. In Fig.7(c) we have an average occupancy $N < 3$ and the resonance is again not visible. The results from sample 2 shown in Fig.7 verify the theoretical model described above.

VI. Summary

A sharp drop in the circular polarization of light emitted by InAs QD based Fe spin-LEDs has been observed for a narrow range of magnetic fields around 5 T. This behavior is attributed to the existence of a magnetic-field dependent electron spin-relaxation mechanism that operates efficiently for these magnetic field values. In order to understand these results we proposed a model that describes an efficient electron spin-relaxation mechanism for an average occupation of three electron-hole pairs per QD. The

prediction of the model was verified in a spin-LED in which we can control the average occupancy of the QDs by varying the device current. When the average number of electron-hole pairs per QD is equal to three we observe the predicted resonance; for average occupancy above and below three no resonance is observed.

Acknowledgments: This work was supported by core programs at NRL and by the Office of the Naval Research Contract No. N0001410WX30262. Work at SUNY Buffalo was supported by NSF grant ECCS0824220 and ONR grant N000140910113. A. Petrou acknowledges support through the Moti Lal Rustgi professorship. M. Korkusinski acknowledges support from the NRC-NSERC-BDC Nanotechnology project and discussions with P. Hawrylak.

References

1. D. Loss and D.P. Divincenzo, Phys. Rev. A **57**, 120 (1998).
2. A.V. Khaetskii and Y.V. Nazarov, Phys. Rev. B **61**, 12639 (2000).
3. Y. Chye, M. E. White, E. Johnston-Halperin, B. D. Gerardot, D. D. Awschalom, and P. M. Petroff, Phys. Rev. B **66**, 201301 (2002)
4. S. Ghosh and P. Bhattacharya, Journal of Vacuum Science & Technology B **20**, 1182 (2002).
5. S. Chakrabarti, M. A. Holub, P. Bhattacharya, T. D. Mishima, M. B. Santos, M. B. Johnson, and D. A. Blom, Nano Lett. **5**, 209 (2005).
6. W. Loffler, D. Trondle, J. Fallert, H. Kalt, D. Litvinov, D. Gerthsen, J. Lupacac-Schomber, T. Passow, B. Daniel, J. Kvietkova, M. Grun, C. Klingshim, and M. Hetterich, Appl. Phys. Lett. **88**, 062105 (2006).
7. M. Ghali, R. Arians, T. Kummell, G. Bacher, J. Wensch, S. Mahapatra, and K. Brunner, Appl. Phys. Lett. **90**, 093110 (2007).
8. J. Seufert, G. Bacher, H. Schomig, A. Forchel, L. Hansen, G. Schmidt, and L. W. Molenkamp, Phys. Rev. B **69**, 035311 (2004).
9. G. Itskos, E. Harbord, S. K. Clowes, E. Clarke, L. F. Cohen, R. Murray, P. Van Dorpe, and W. Van Roy, Appl. Phys. Lett. **88**, 022113 (2006).
10. C. H. Li, G. Kioseoglou, O. M. J. van 't Erve, M. E. Ware, D. Gammon, R. M. Stroud, B. T. Jonker, R. Mallory, M. Yasar, and A. Petrou, Appl. Phys. Lett. **86**, 132503 (2005).
11. L. Lombez, P. Renucci, P. F. Braun, H. Carrere, X. Marie, T. Amand, B. Urbaszek, J. L. Gauffier, P. Gallo, T. Camps, A. Arnoult, C. Fontaine, C.

- Deranlot, R. Mattana, H. Jaffres, J. M. George, and P. H. Binh, *Appl. Phys. Lett.* **90**, 081111 (2007).
12. G. Kioseoglou, M. Yasar, C. H. Li, M. Korkusinski, M. Diaz-Avila, A. T. Hanbicki, P. Hawrylak, A. Petrou, and B. T. Jonker, *Phys. Rev. Lett.* **101**, 227203 (2008).
 13. A. T. Hanbicki, B. T. Jonker, G. Itskos, G. Kioseoglou, and A. Petrou, *Appl. Phys. Lett.* **80**, 1240 (2002).
 14. A. T. Hanbicki, O. M. J. van 't Erve, R. Magno, G. Kioseoglou, C. H. Li, B. T. Jonker, G. Itskos, R. Mallory, M. Yasar, and A. Petrou, *Appl. Phys. Lett.* **82**, 4092 (2003).
 15. E. A. D. E. Silva, G. C. LaRocca and F. Bassani, *Phys. Rev. B* **55**, 16293-16299 (1997)
 16. M. Korkusinski and P. Hawrylak, *Phys. Rev. Lett.* **101**, 027205 (2008).
 17. P. Hawrylak, *Phys. Rev. B* **60**, 5597 (1999).
 18. M. Florescu and P. Hawrylak, *Phys. Rev. B* **73**, 045304 (2006).
 19. R. Heitz, H. Born, A. Hoffmann, D. Bimberg, I. Mukhametzhanov, and A. Madhukar, *Appl. Phys. Lett.* **77**, 3746 (2000).
 20. D. V. Bulaev and D. Loss, *Phys. Rev. B* **71**, 205324 (2005).
 21. P. Stano and J. Fabian, *Phys. Rev. B* **74**, 045320 (2006).
 22. H. Kosaka, A. A. Kiselev, F. A. Baron, K. W. Kim, and E. Yablonovitch, *Electronics Lett.* **37**, 464 (2001).
 23. T. Nakaoka, T. Saito, J. Tatebayashi, S. Hirose, T. Usuki, N. Yokoyama, and Y. Arakawa, *Phys. Rev. B* **71**, 205301 (2005).

Figure Captions:

Fig.1: Circular polarization of Sample 1 plotted as function of magnetic field at $T = 7$ K. Inset: Electroluminescence from Sample 1 at $I = 5$ mA (black line). The green and red lines represent a deconvolution into two features attributed to the s- and p-shells at 1.222 and 1.267 eV, respectively.

Fig.2:

a. Circular polarization of the light emitted by Sample 1 plotted versus magnetic field at $T = 7$ K for $I = 0.3, 1$ and 5 mA.

b. Circular polarization of the light emitted by Sample 1 plotted versus magnetic field at $T = 7, 15, 30, 45,$ and 50 K; $I = 1$ mA

Fig.3:

a) Low spin ground state, A, of the 3X system

b) High spin excited state, B, of the 3X system

c) Low spin excited state, C, of the 3X system.

Fig.4: Calculated energies E_A, E_B, E_C of the 3X system for states A, B, and C, respectively, plotted as function of magnetic field B .

Fig.5:

a) Low spin ground state, A, of the 2X system

b) High spin, $L = -1$ excited state, B, of the 2X system

c) High spin, $L = 0$ excited state, C, of the 2X system.

Fig.6: Electroluminescence from Sample 2, recorded at $T = 7$ K, $B = 0$ T with the biasing adjusted so that average occupation N of the QDs for electrons and holes is equal to 3.

Fig.7: Circular polarization of the light emitted by Sample 2 plotted versus magnetic field B at $T = 7$ K. a) $N > 3$, b) $N = 3$, and c) $N < 3$

Fig.1

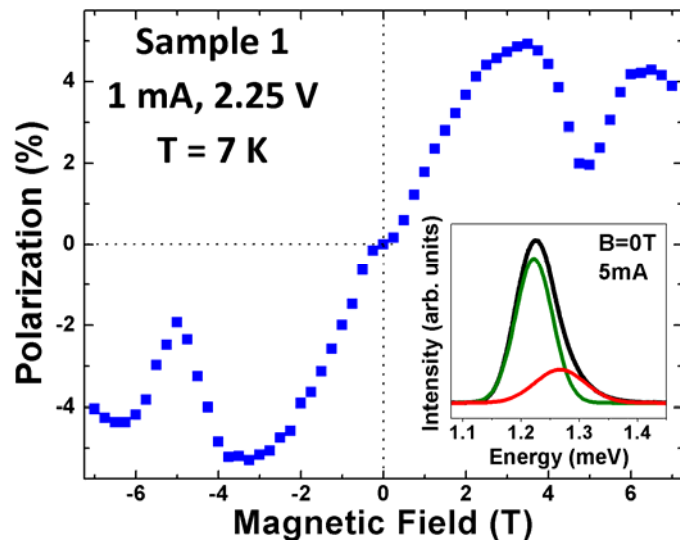


Fig.2

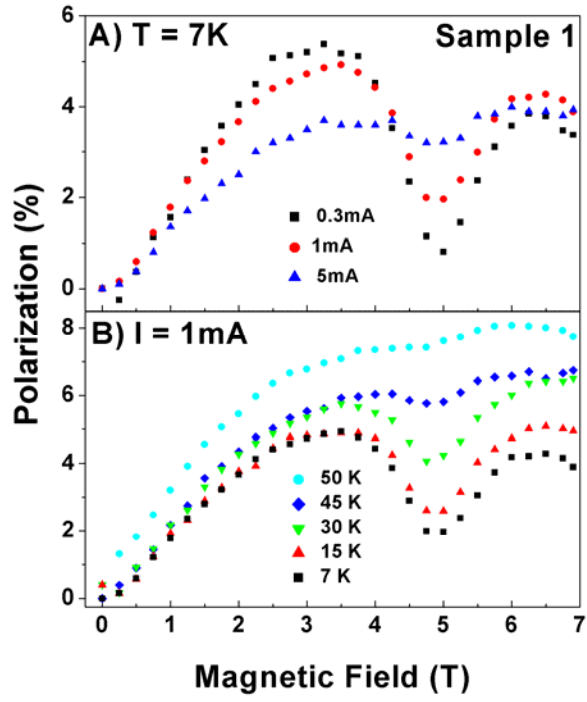


Fig.3

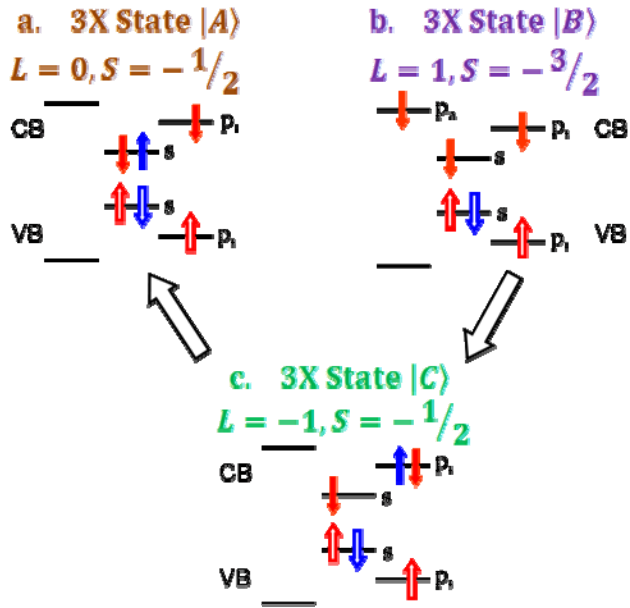


Fig.4

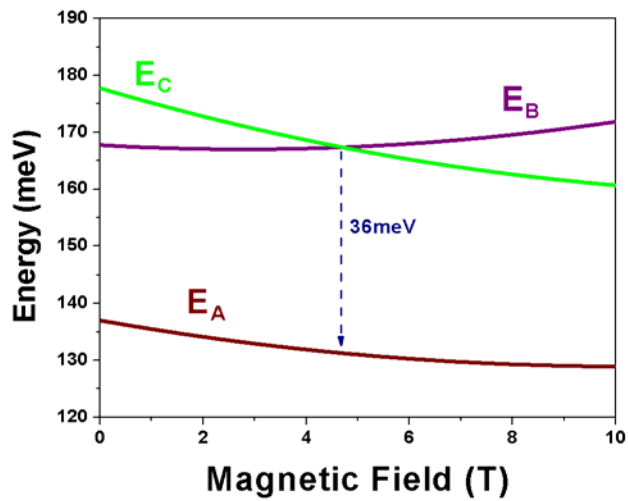


Fig.5

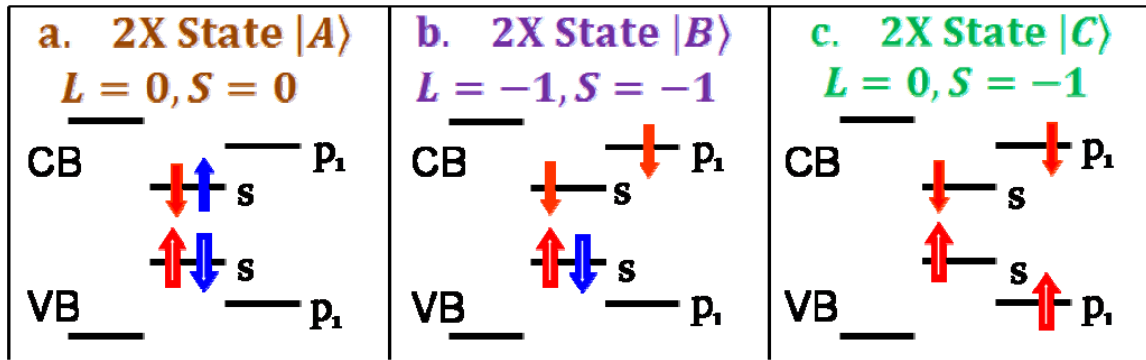


Fig.6

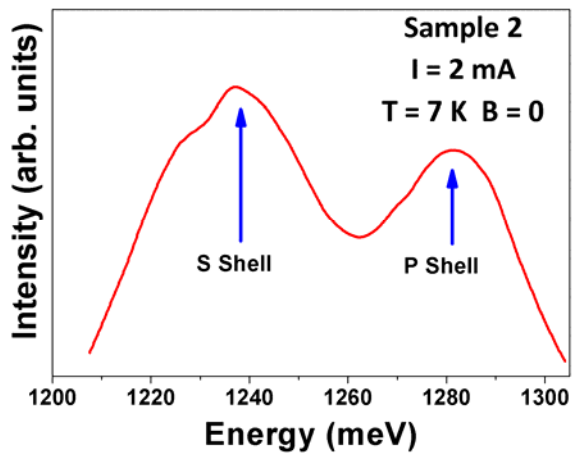


Fig.7

